ELSEVIER

Earth and Planetary Science Letters 163 (1998) 149–165

EPSL

High geothermal gradient metamorphism during thermal subsidence

Mike Sandiford *, Martin Hand, Sandra McLaren

Department of Geology and Geophysics, University of Adelaide, Adelaide, S.A. 5005, Australia

Received 22 December 1997; revised version received 13 July 1998; accepted 25 August 1998

Abstract

The burial of a basement sequence enriched in heat producing elements during thermal subsidence following rifting produces two concomitant changes in the thermal structure of the crust. Firstly, the burial of the enriched layer produces high geothermal gradients in the overlying sedimentary succession, with the high gradients propagating down into, but not through, the enriched basement sequence. Secondly, the lithospheric thickening that drives thermal subsidence reduces the heat flowing into the deeper crust from the mantle. Because the process of thermal subsidence promotes burial, it naturally increases the depth extent of the high geothermal gradients in the upper crust, potentially inducing significant temperature increases in the mid-upper crust during burial. The lowering of the thermal gradients in the deep crust accompanying burial severely limits the temperature changes affecting the Moho; potentially allowing Moho cooling while the mid-upper crust heats. These effects can promote high geothermal gradient ($>40^{o}$C/km) metamorphism in the mid-upper crust without inducing significant melting in the lower crust, providing the basement heat production contributes $> \sim 70$ mW m^{-2} to the surface heat flow and that the horizontal length scale for the basement heat production anomaly is $> \sim 50$ km. These conditions appear to be met in several Australian intermediate- to high-temperature, low-pressure metamorphic terranes where the thermal causes of metamorphism have hitherto remained enigmatic. One of these terrains, the Mt. Painter province in the northern Flinders Ranges, South Australia, is used to illustrate some of the attributes of the model.

Keywords: geothermal gradient; metamorphism; subsidence

1. Introduction

The thermal energy that drives metamorphism is ultimately related to the processes of heat loss from the interior of the earth. As such, metamorphism must be seen as a consequence of the conductive and advective heat transfer phenomena associated with lithospheric processes such as deformation, erosion and magma transport. Metamorphism at gradients in excess of about 40^{o}C/km results in intermediate- to high-temperature, low-pressure metamorphism in the middle crust. The physical causes of such high geothermal gradient metamorphism (HGGM) have received considerable attention in recent years with much of the emphasis on the role of transient advective processes such as magma ascent, or abnormally high heat flows from the mantle (e.g. [1–7]). Because the generation of magmas in the deep crust and upper mantle is associated with anomalously steep thermal gradients, it is clear that HGGM metamorphism in the shallower parts of the lithosphere

* Corresponding author. Fax: 0061 8 8303 4347; E-mail: msandifor@geology.adelaide.edu.au

0012-821X/98/$ – see front matter
PII: S0012-821X(98)00183-6

may be produced by a combination of advective processes associated with the segregation and ascent of magmas within the lithosphere and enhanced heat flow from the mantle. Indeed, the spatial correlation between metamorphism and magmatism in many high temperature metamorphic belts has been used to support hypothesis [1,6,7]. Rapid tectonic denudation of deep crust provides a further mechanism for generating HGGM, albeit transiently, and has been proposed as a mechanism for the production of some localised high-temperature metamorphic terranes in modern orogenic belts such as the Nanga Parbat massif [8,9].

While this notion of transient advection remains the principal paradigm for HGGM, several recent thermochronologic studies have raised the possibility that other less transient mechanisms may play a significant or even dominant role. For example, evidence for extended periods of HGGM, with the elevated geothermal regimes apparently lasting many 10s of millions of years (e.g. [10–12]), precludes a predominant advective mode. In several Australian HGGM terranes with prima facie evidence for magmatic advection of heat (in as much as metamorphism is spatially associated with granitic batholiths), recent geochronological studies have shown that the HGGM metamorphism postdates the emplacement of the batholiths by more than 100 Myr [12–14]. These results seem to preclude metamorphism being driven primarily by magmatic activity or rapid tectonic denudation (based on the retrograde P–T paths), raising the questions about the physical cause(s) of the high geothermal gradients associated with the HGGM metamorphism. A specific difficulty relating to HGGM metamorphism in the absence of magmatism (and rapid denudation) is how steep geothermal gradients are sustained in the mid-upper crust, while temperatures in the deep crust are sufficiently low to inhibit large scale melting.

In the absence of advective heat transfer processes, metamorphism must represent the conductive response to burial of rocks with the elevated geotherms associated with HGGM reflecting either unusually elevated heat production in the crust, and/or high heat flows from the mantle. The role of high mantle heat flows has been addressed by a number of authors [2,3]. However, as alluded to above it is difficult to generate conductive thermal regimes appropriate to HGGM at mid-crustal levels by enhancing mantle heat flows without generating significant quantities of magma in the deeper crust, with the likely result that the advection of the generated magma would contribute to the observed HGGM signature. In the context of HGGM, the role of anomalous crustal heat production [15] remains poorly understood because of relatively entrenched, somewhat conservative views about the magnitude of crustal heat production in some instances and the way in which it is distributed within the lithosphere.

Sandiford and Hand [16] have shown that heat production distributions consistent with modern heat flows and measured surface heat production in a number of Australian Proterozoic HGGM terranes, can generate the conditions required for HGGM in the mid-upper crust without necessarily generating significant quantities of melt in the deep crust (provided mantle heat flows are low). Sandiford and Hand's [16] approach was essentially parametric in as much as they did not address the geological setting in which such conditions are likely to prevail. In this contribution we develop a coupled thermal-isostatic model to show that such conditions will naturally develop as a consequence of burial of a radioactive sequence (such as a granitic basement complex) during thermal subsidence following rifting. The motivation for this analysis is provided by the geological evolution of the Mount Painter province in the northern Flinders Ranges, South Australia, which we discuss in the context of this scenario. We believe that the geology of the Mount Painter region may have bearing on the origin of HGGM metamorphism in other settings in the Proterozoic of Australia, and we briefly discuss aspects of selected Australian Proterozoic terrains that may be resolved by this new view of HGGM metamorphism.

Because thermal subsidence following rifting is normally associated with crustal cooling (Fig. 1a–c), the suggestion that HGGM may result from thermal subsidence is somewhat counter-intuitive. Consequently, we spend some time developing an insight into the basic physics of the 'HGGM during thermal subsidence' scenario. We begin with a short summary of the physical arguments for the thermal subsidence scenario for HGGM, before outlining a simple model of heat production that allows quantification of the scenario.

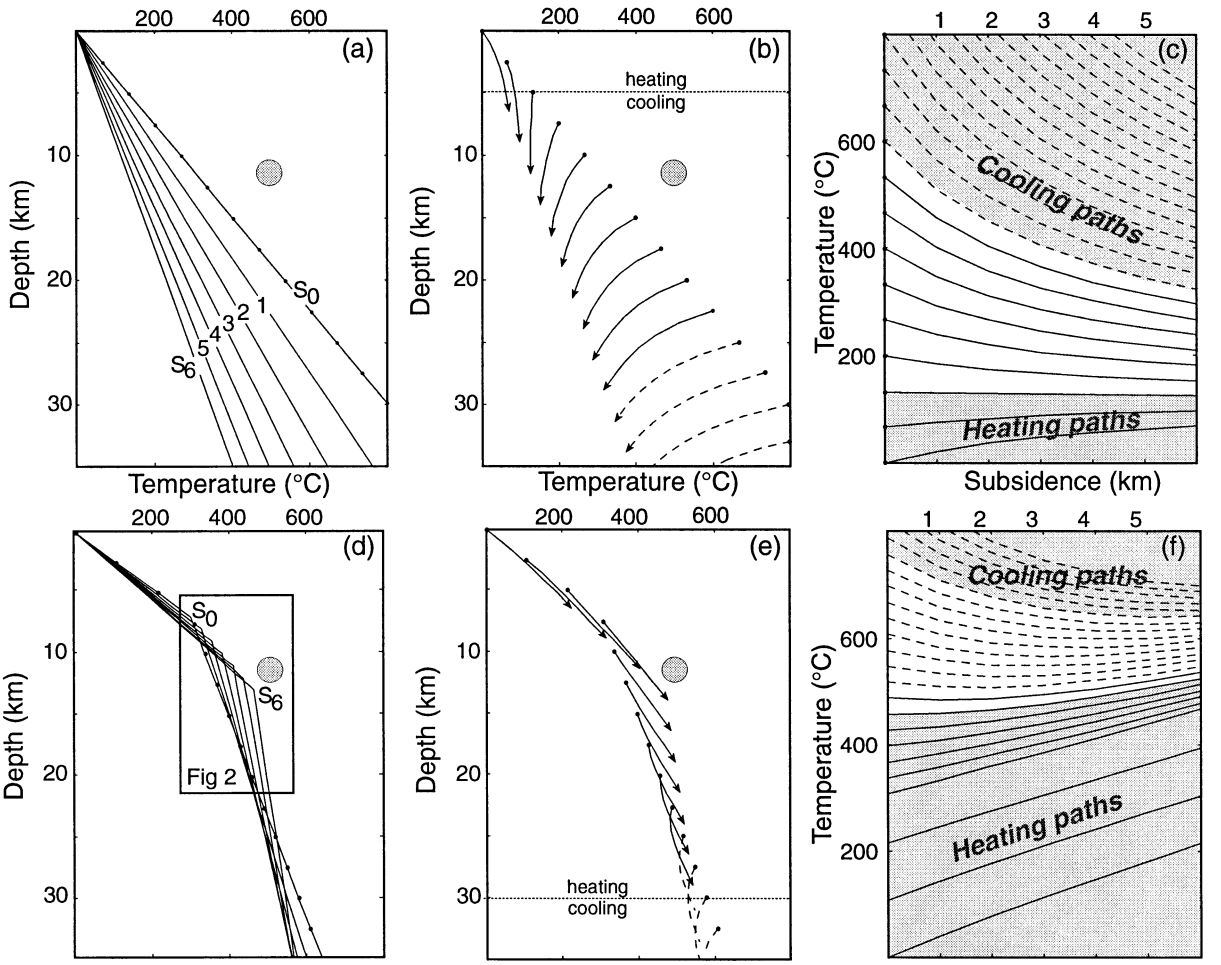

Fig. 1. (a–c) Since thermal subsidence is driven by cooling and consequent densification of the mantle lithosphere it is normally associated with crustal cooling. This notion is (and has frequently been) highlighted by isostatic models that ignore heat production in the crust. For this case geotherms are linear functions of depth, tending to lower gradients with increasing subsidence (or time). Fig. 1a shows the geotherms associated with thermal subsidence following rifting of a lithosphere initially 125 km thick and which contains no internal heat production. The rifting is assumed to be distributed homogeneously across the lithosphere with the stretching factor enough to allow accumulation of 6 km of sediment during the ensuing thermal subsidence (that is after 6 km of subsidence, the lithosphere has returned to its initial thickness of 125 km). Geotherms are shown at the onset of subsidence ($s = 0$) and for each kilometre of subsidence ($s = 1$ to 6). The circle shows the metamorphic conditions in the Mt. Painter Inlier which is discussed in a following section. Fig. 1b shows the temperature–depth paths of individual material points spaced at 2.5 km increments through the crust and upper mantle, while Fig. 1c shows the temperature paths for these same points as a function of subsidence (note that while subsidence can be used as a proxy for time, the subsidence axis does not scale linearly with time, but rather to the square root of time). Fig. 1b and c show that, in the case where internal heat production is ignored, all but the upper few kilometres of the crust witnesses cooling during thermal subsidence. These upper few kilometres of the crust are heated by virtue of role played by burial during subsidence. The transition point from heating to cooling occurs at initial depths of about 5 km (final depths of ~11 km) and at temperatures of <200ºC. (d–f) Illustration of the geothermal evolution of the crust during thermal subsidence incorporating heat production into the crust in a discrete thin layer ($q_c = 70$ mW m^{-2}). The kink in the geotherm marks the position at which the heat production is concentrated, with this kink migrating to deeper levels with progressive subsidence (for greater is concentrated, with this kink migrating to deeper levels with progressive subsidence (for greater detail see Fig. 2). Note the transition depth from overall heating to overall cooling paths is now at ~30 km corresponding to temperatures of ~600ºC. Points between ~22 and 30 km initially cool, but subsequently undergo heating toward the end of the subsidence. These figures, together with Fig. 4, illustrate that the effect of crustal heat production is to significantly increase the temperatures and depths of the transition point between heating and cooling paths during thermal subsidence, thus allowing the possibility of heating rocks into the field appropriate to HGGM during progressive subsidence. Dashed lines imply mantle, while solid lines imply crust.

2. HGGM due to high crustal heat production and low mantle heat flow

The main problem presented by HGGM metamorphism in the absence of advective heat transfer is the question of how high geothermal gradients are sustained in the upper crust without inducing melting in the deep crust. A useful starting point for understanding this problem is provided by an analysis of steady-state thermal structure of the lithosphere. We begin by making the simplifying assumption that the lithosphere is laterally uniform and by ignoring compositional and temperature dependence on thermal conductivity. Under these circumstances the absolute value of the heat flow at any depth, z, is sum of the heat flow contributed by the deeper mantle ($\bar{q}_m$) and the heat production contributed by lithospheric sources beneath that depth:

$$\bar{q}(z) = \bar{q}_m + \int_{z_l}^{z} H(z)\,dz \quad (1)$$

The integral term in Eq. 1 leads to an inverse correlation between absolute heat flow and depth, and to the characteristic curvature of continental geotherms. Because heat-producing elements tend to be enriched in the upper parts of the lithosphere, in the mid- to upper crust, lithospheric geotherms are likely to be most strongly curved in the near surface.

Sandiford and Hand [16] have shown that the combination of high geothermal gradients in the upper crust, and lower crustal temperatures beneath the bulk crustal solidus, imposes specific constraints on the thermal parameter distributions of the crust. For thermal conductivities of 2–3 W m^{-1} K^{-1}, the relevant parameter range involves crustal heat production strongly concentrated at mid-crustal levels (10–20 km depth) contributing in excess of ~70 mW m^{-2} (when integrated over the thickness of the enriched segment) and low–intermediate mantle heat flows (10–20 mW m^{-2}). While such high heat production values may be considered to be extreme, and are probably unusual, Sandiford and Hand [16] have shown that such a distribution is consistent with observed heat production–heat flow regimes in a number of Proterozoic HGGM metamorphic belts in Australia. For example, in the HGGM Proterozoic terranes that dominate the central part of the Australian continent, the modern day heat flow averages ~85 mW m^{-2} and locally exceeds 100 mW m^{-2} [17] and must have been even more at the time of metamorphism given that some 10–20 km of denudation has exposed the Proterozoic provinces. Lithospheric thicknesses estimates of the order of 200–300 km throughout this region [18] suggest low contemporary mantle heat fluxes (~10–15 mW m^{-2}) implying crustal heat sources contribute in excess of 70 mW m^{-2} to the average measured heat flow. Across much of this region near surface temperature gradients determined from drill hole measurements are in excess of 35ºC/km [19] leading further support to the notion that substantial heat production is concentrated in the crust. Granitic gneisses, which commonly comprise more than 50% of the basement terrains in these Proterozoic belts are unusually good heat producers, and frequently have heat production rates in the range 5–10 μW m^{-3}. During metamorphism in the Proterozoic and Phanerozoic, these basement sequences were buried to depths of 10–20 km, thus providing an ideal mid-crustal radioactive sequence of the type alluded to here. We note that the implied crustal heat production contribution for these parts of the Australian lithosphere contrast markedly with conventional wisdom as expressed, for example, by McLennan and Taylor [20] who state “the crustal radiogenic component of continental heat flow must lie in the range 18–48 mW m^{-2}”.

3. HGGM metamorphism and thermal subsidence

While Sandiford and Hand [16] demonstrated the plausibility of HGGM metamorphism using parameter ranges consistent with constraints imposed by known surface heat flow–heat production data, they did not address the question of geologic setting that enables establishment of the appropriate heat production distributions and mantle heat flows. One way of achieving the requirements of elevated heat production at mid-crustal levels accompanied by low mantle heat flows is to bury an enriched sequence, such as granitic basement, beneath a thick sedimentary succession during thermal subsidence following a rift basin forming episode. In this context the importance of thermal subsidence is twofold: (a) it serves to increase the depth to which steep upper

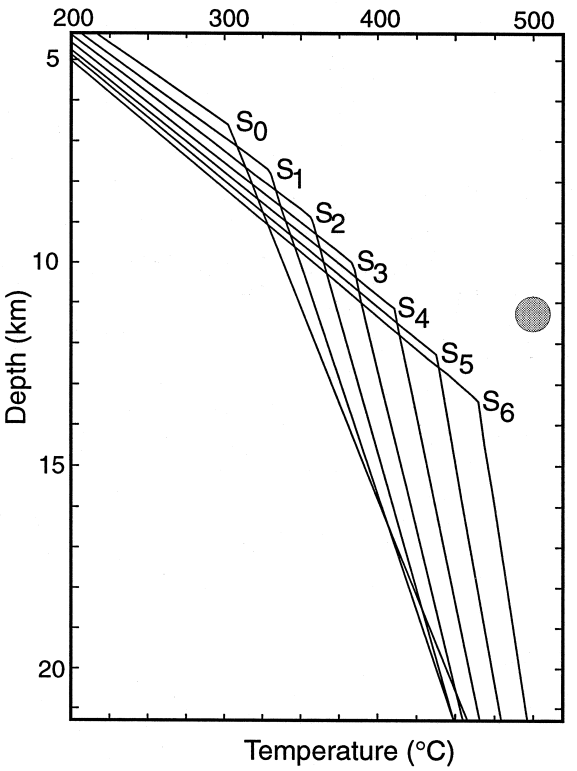

Fig. 2. Details of Fig. 1d, showing the kink in the geotherm associated with the discrete heat production horizon.

crustal geothermal gradients propagate within the lithosphere; and (b) the reduction in heat flowing from the deep lithosphere, $\bar{q}_m$, reduces geothermal gradients in the deep crust as the basement sequence is progressively buried, thus serving to limit the temperature changes in the deep crust.

An insight into this scenario which preserves all the essential physics is provided by a simplistic model in which all the heat production in the crust is concentrated in a line source at depth z_i beneath an accumulating sedimentary succession. Such a concentration produces a prominent kink in the geotherm which separates a high gradient segment above from a low gradient segment below (see Figs. 1 and 2). In this scenario the absolute value of the heat flow at the surface, $\bar{q}_s$, is given by the sum of the crustal heat production, q_c, concentrated in the enriched layer, and the absolute value of the heat flowing from the deeper lithosphere, $\bar{q}_m$:

$$\bar{q}_s = q_c + \bar{q}_m \frac{kT_i}{z_i} \quad (2)$$

where T_i is the temperature at the depth z_i and k is the thermal conductivity taken here to be temperature and depth independent. For a thermally stabilised lithosphere with a lower boundary condition defined by a constant temperature ($T_l = 1300$ºC), $\bar{q}_m$ can be defined as:

$$\bar{q}_m = k \frac{T_l - T_i}{z_l - z_i} \quad (3)$$

Solving for T_i and $\bar{q}_s$ in terms of k, z_i and q_c yields:

$$T_i = z_i \frac{kT_l - q_c z_i + q_c z_l}{kz_l} \quad (4)$$

$$\bar{q}_s = \frac{kT_l - q_c(z_i + z_l)}{z_l} \quad (5)$$

Provided that the enriched horizon contributes in excess of about 70 mW m^{-2} then upper crustal thermal gradients will exceed 40ºC/km. The exact value of the upper crustal geotherm will depend on the conductivity of the upper crust (Fig. 3b) and, to a lesser extent, the thickness of the lithosphere (Fig. 3a). For the scenario considered below where burial of a radioactive sequence occurs in response to deposition of sediments during thermal subsidence, we can assume relatively low thermal conductivities within the accumulating sedimentary pile (e.g., [21,22]). In the calculations below we use, for want of better constraints, a reference value for thermal conductivity of 2.25 W m^{-1} K^{-1}. We note, however, that the sensitivity of the thermal gradients to the thermal conductivity structure of a sedimentary succession implies a first order control which remains poorly constrained (and is more than likely quite variable from place to place).

During rifting and the ensuing thermal subsidence, sedimentation is driven by isostatic depression of the surface of the attenuated lithosphere (e.g., [23]). The syn-rift subsidence is dominated by density defects induced by crustal thinning, while the thermal subsidence is related to cooling and associated densification of the attenuated lithospheric mantle following active rifting (Fig. 1b). The coupling between sedimentation and lithospheric thermal evolution during the thermal subsidence is readily achieved by assuming isostatic balance at the

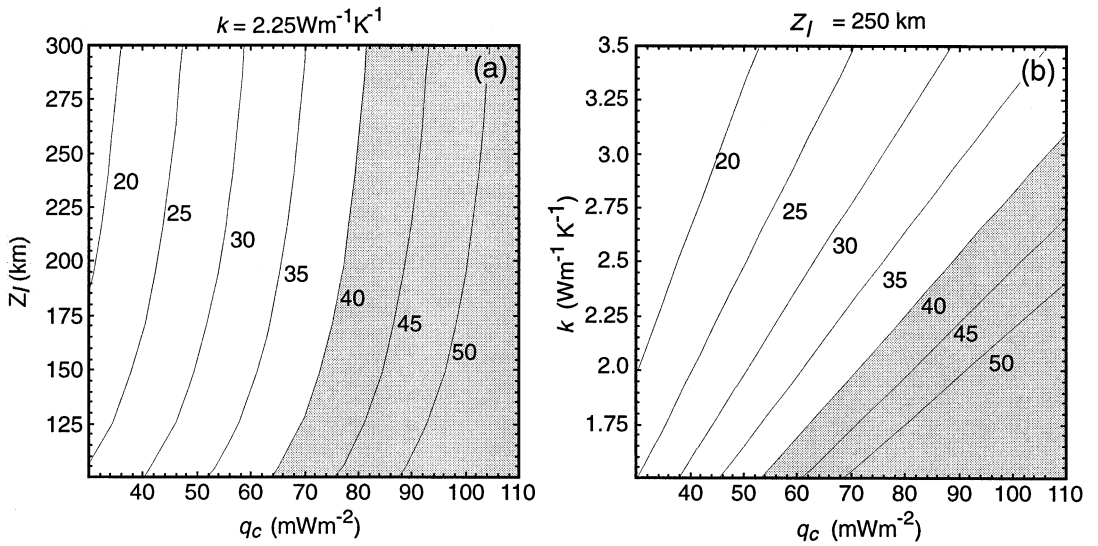

Fig. 3. Dependence of crustal thermal gradients at depths less than the heat production anomaly (z_i = 13 km), on (a) crustal heat production (q_c) and lithospheric thickness (z_l) and (b) thermal conductivity (k) and crustal heat production. Note that upper crustal thermal gradients in excess of ~40ºC/km (shaded region) as required for HGGM are only possible for $q_c > \sim$ 65 m W m^{-2}. Contours in ºC/km.

depth appropriate to the pre-rift lithospheric thickness, i.e.:

$$\int_0^{z_l} (\sigma_{zz})_{\text{reference}}\, dz = \int_0^{z_l} (\sigma_{zz})_{\text{subsidence}}\, dz \qquad (6)$$

In the following calculations we assume that the thermal subsidence restores the lithosphere to the initial (or pre-rift thickness). The crust is initially 30 km thick (see Table 1 for default thermal parameters). Fig. 1d–f and 2 illustrate the thermal evolution for a lithosphere during subsidence with this artificially concentrated heat production (q_c = 70 mW m^{-2}). Geotherms are shown appropriate to thermal subsidence at 1 km intervals with the initial rifting sufficient to produce a thermal subsidence of 6 km (assuming sediment fill). The heat production concentration is assumed to be at depth of 7 km prior to thermal subsidence, as might be appropriate to a basement sequence buried by a thick syn-rift sequence. Following thermal subsidence, the heat production concentration is at 13 km depth. The obvious characteristic of the geotherms shown in Fig. 2

Table 1
List of symbols along with default values used in calculations

Symbol	Description	Default value
z_l	Lithospheric thickness	175–250 km
z_c	Crustal thickness	30 km
z_i	Depth of heat production maxima	Initially 7 km
k	Thermal conductivity	2.25 W m^{-1} K^{-1}
q_c	Vertically integrated crustal heat source contribution	70 mW m^{-2}
q_m	Mantle heat flow	Not prescribed
α	Coefficient of thermal expansion	3 × 10^{-5} K^{-1}
ρ_c	Reference crust density	2700 kg m^{-3}
ρ_m	Reference mantle density	3300 kg m^{-3}
hz_r	Characteristic vertical length-scale for heat production	5 km
hx_r	Characteristic horizontal length-scale for heat production	Variable

is the kink at depth z_i at which the heat production is concentrated. With increasing subsidence this kink migrates to deeper levels, along an upper crustal geotherm gradient given by $(q_c + q_m)/k$. The fact that thermal subsidence is driven by a reduction in the mantle heat flow, q_m, is evident in the dramatic decrease in the thermal gradient beneath z_i with increasing sedimentation. Since the surface heat flow is dominated by crustal heat sources (i.e., q_c), the decline in q_m with subsidence causes only a small decline in the near surface geotherm through time (Fig. 3).

While the heat production model used above illustrates the essence of the scenario outlined here, it is obviously unrealistic to view the crustal heat production as concentrated at a single horizon. The notion of a buried, high heat production horizon can easily be extended more generally using a form of heat production modified from the exponential model of Lachenbruch [32] and others:

$$H(z) = H_i \exp\left(\frac{-(z - z_i)^2}{hz_r^2}\right) \quad (7)$$

In this distribution $H(z)$ varies with depth reaching its maximum value H_i at depth z_i. The parameter hz_r provides a measure of the vertical spread of the heat production with the heat production falling to $H_i e^{-1}$ at depths $z_i \pm h_r$. As discussed by Sandiford and Hand [16] this model appears broadly consistent with modern heat flow–surface heat production data in a number of HGGM terranes in Australia.

Fig. 4 shows the thermal evolution of a number of scenarios using this form of heat production distribution. The four cases illustrated in Fig. 4 differ in the total amount of heat produced by the crust (q_c = 30, 50, 70 and 90 mW m^{-2}), and in the assumed reference thickness of the lithosphere (z_l = 175, 200, 225 and 250 km). One of the side effects of increasing the heat production in the crust is the reduction in the amount of thermal subsidence induced by a given stretching factor. In order to explore the effects of varying crustal heat production with a uniform subsidence (in this case 6 km) it has, therefore, been necessary to vary the initial thickness of the lithosphere. In our calculation we use an initial lithospheric thickness that, on stretching, yields similar 'syn-rift' geotherms independently of the total crustal heat production (see Fig. 4).

Fig. 4 illustrates the important control exerted by heat production on the transition depth from net heating to net cooling paths. This transition depth varies from about 15 km at q_c = 30 mW m^{-2} (or temperature equivalent of ~300ºC) to greater than 25 km for q_c = 90 mW m^{-2} (temperature equivalent of ~650ºC). Temperature–subsidence paths near the transition point show initial cooling associated with the reduction in q_m, followed by heating due to the burial of the high heat producing layer. Importantly, Fig. 4g and 4l show that for $q_c >\sim$ 60 mW m^{-2} not only do most crustal P–T paths show heating during subsidence but that progressive subsidence accesses realms of P–T space not previously encountered by any parts of the crust in the earlier P–T evolution. In other words, prograde metamorphism is a logical outcome during thermal subsidence for $q_c >\sim$ 60 mW m^{-2}.

4. 2-D variation in heat sources

An implicit assumption in the 1-D modelling presented in the previous section is that the distribution of heat sources at any depth is laterally invariant, at least for length scales large in comparison to the thickness of the lithosphere. This is a geologically implausible scenario for two reasons. Firstly, the extreme concentrations of heat sources needed to generate HGGM during thermal subsidence are only likely to occur as localised enrichments. Secondly (and perhaps more importantly), assuming that the anomalous heat production was located in the upper crust, then the rifting that preceded thermal subsidence is likely to result in its heterogeneous attenuation. The natural length-scales for such attenuation are in the range 10–100 km. In this section we address the role of lateral variations in heat production, by using finite element models appropriate to the burial of a laterally confined heat producing layer. We adopt a variation of the heat production distribution used for the 1-D case to describe a spatially localised heat production anomaly:

$$H(x, z) = H_i \exp\left(\frac{-(z - z_i)^2}{hz_r^2}\right) \exp\left(\frac{-x^2}{hx_r^2}\right) \quad (8)$$

where hz_r and hx_r are the characteristic length scales of the heat production anomaly in the vertical and

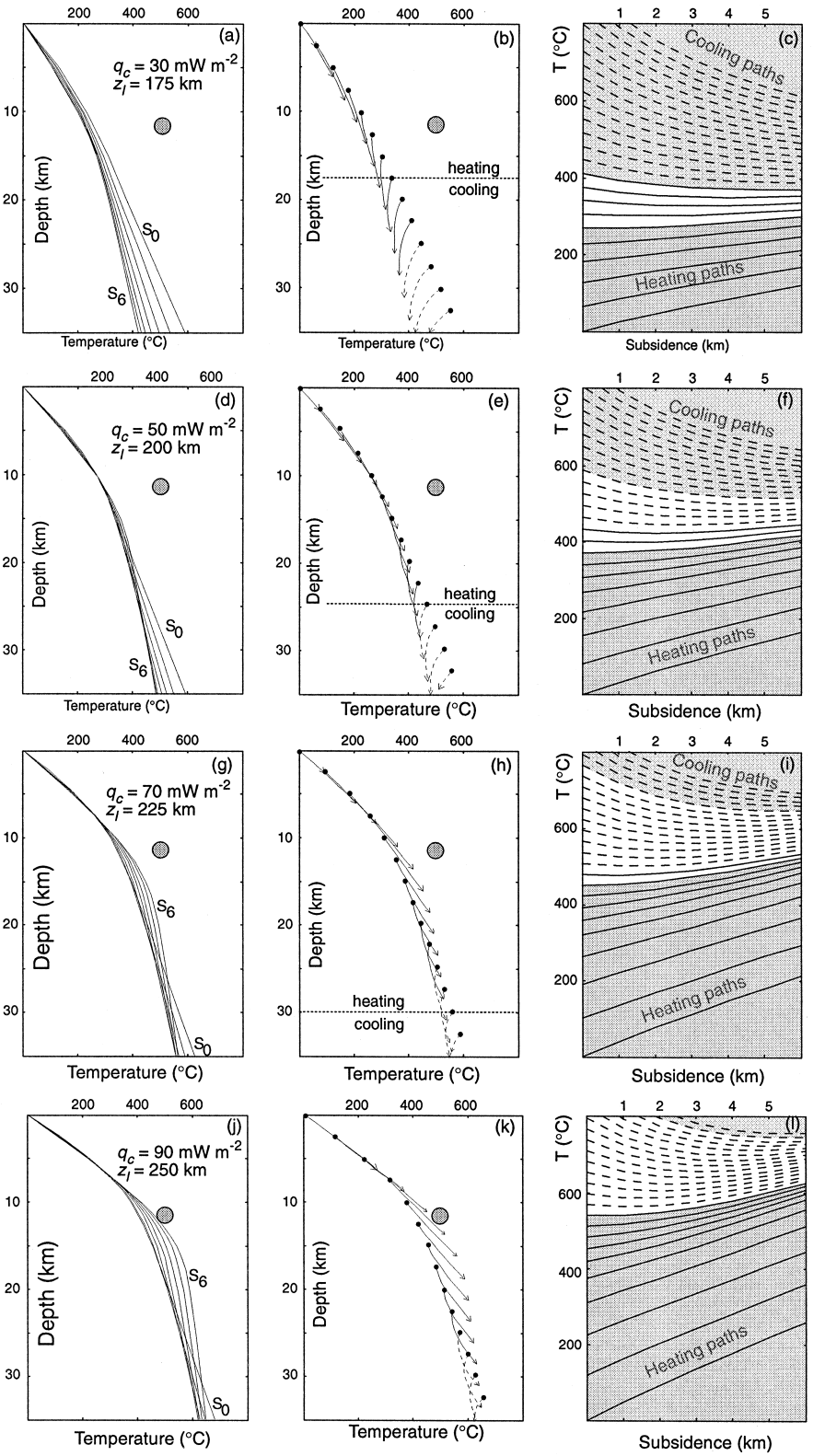
(a)
q_c = 30 mW m^{-2}
z_l = 175 km
(b)
heating
cooling
(c)
Cooling paths
Heating paths
(d)
q_c = 50 mW m^{-2}
z_l = 200 km
(e)
heating
cooling
(f)
Cooling paths
Heating paths
(g)
q_c = 70 mW m^{-2}
z_l = 225 km
(h)
heating
cooling
(i)
Cooling paths
Heating paths
(j)
q_c = 90 mW m^{-2}
z_l = 250 km
(k)
(l)
Heating paths
Depth (km)
Temperature (°C)
T (°C)
Subsidence (km)
S_0
S_6

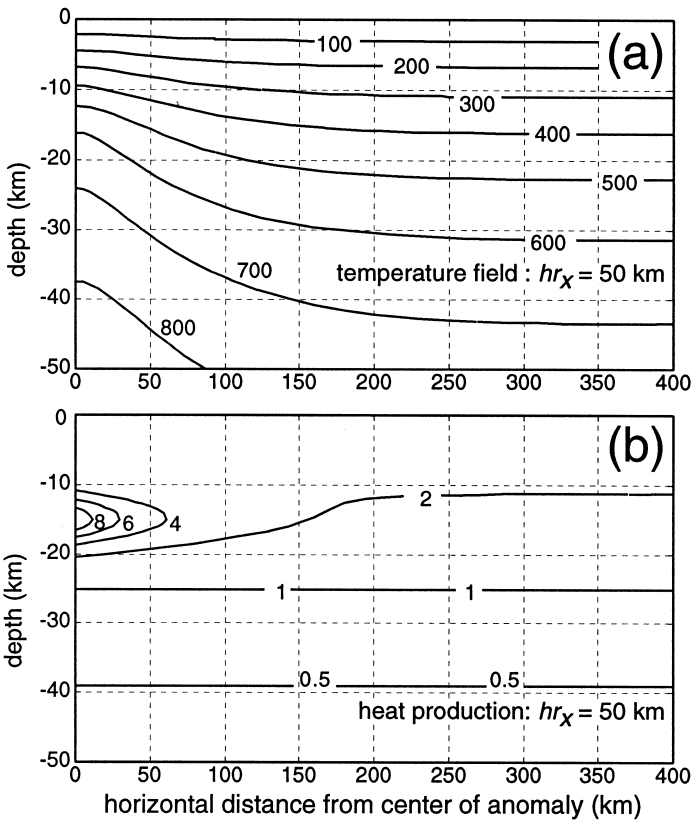

Fig. 5. (a) 2-D thermal model for a laterally confined heat production distribution as given by Eq. 8 with $hx_r = 50$ km (and as shown in (b)). Model parameters are such that the background contribution to crustal heat production is 60 mW m^{-2}, with the heat production anomaly contributing an additional 50 mW m^{-2}. The lithospheric thickness is set to 200 km producing a maximum reduced heat flow of about 10 mW m^{-2}. Heat production contours are in μW m^{-3}.

horizontal directions, respectively. This distribution is superimposed on a more regular laterally invariant heat production distribution as shown in Fig. 5b, with its resulting thermal structure shown in Fig. 5a. Note that we have only investigated the thermal structure attained following termination of subsidence. Fig. 6 shows the temperature variation (normalised against the solution for the 1-D approximation) directly beneath the centre of the heat production anomaly as a function of the parameter hx_r (the characteristic horizontal length scale). The calculations summarised in Fig. 6 indicate that providing the characteristic length scale of the heat production anomaly is greater than about 50 km, then upper crustal temperatures will be greater than 70% of the theoretical maximum. Fig. 6 also shows that for any given value of hx_r, the normalised temperature decreases with increasing depth, such that for $hx_r = 50$ km the normalised temperature appropriate to Moho depths (i.e., 30–35 km) is some 15% lower than at 10

Fig. 4. 1-D models for thermal subsidence for $q_c = 30$ mW m^{-2} and z_l (ref) = 175 km (a–c), 50 mW m^{-2} and z_l (ref) = 200 km (d–f), 70 mW m^{-2} and z_l (ref) = 250 km (j–l). The transition from net cooling to net heating paths increases from ~15 km with $q_c = 30$ mW m^{-2} to ~30 km with $q_c = 90$ mW m^{-2}. Fig. 4j shows the metamorphic conditions in the Mt. Painter Inlier (circle) see text for details) are approached toward the end of subsidence in thick lithosphere containing crust with very high total heat production. Thermal parameter values used in calculations are listed in Table 1. Dashed lines imply mantle, solid lines imply crust.

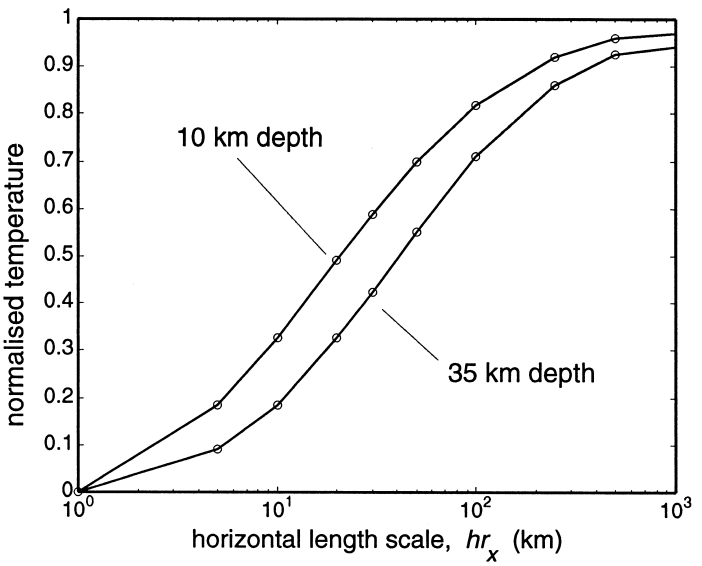

Fig. 6. To illustrate the effect of the horizontal length scale for the heat production anomaly the normalised temperatures are plotted (at depths $z = 10$ and 35 km) immediately beneath the centre of the anomaly as a function of hx_r (see text for discussion). The temperatures are normalised against the solution for the 1-D (infinite sheet) approximation, and thus span a range from 0 at $hx_r = 0$ (i.e., no anomalous heat production) to 1 at $hx_r = \infty$ (i.e., the 1-D solution).

km depth. This relatively increased cooling effect at depth would seem to have particular relevance to the problem of generating HGGM, since it greatly enhances the possibility that steep mid-upper crustal geotherms can exist without the generating excessively high deep crustal temperatures that would lead to large scale melting.

5. Application to the Mount Painter province

In the previous sections we have shown that the burial of an anomalously radioactive crust during thermal subsidence allows the possibility of HGGM metamorphism with the provisos that: (1) the total contribution of the crust is greater than about 70 mW m^{-2}, and (2) the characteristic horizontal length scale of the heat production anomaly is greater than about 50 km. In this section we describe the metamorphism in the Mount Painter province; a terrane that seems to fulfil the above criteria and where we believe a 'thermal subsidence' scenario may be applicable.

The Mount Painter province occurs in the northern Flinders Ranges in South Australia (Figs. 7 and 8). It consists of two inliers (the Painter and Babbage Inliers) comprising Mesoproterozoic (~1500–1600 Ma) granitic gneisses and metasediments exposed over ~780 km^2. The basement gneisses are overlain by a thick (~7–12 km) Neoproterozoic sedimentary succession forming part of the Adelaide geosyncline. The Neoproterozoic cover succession was deposited over some ~270 Myr (800–530 Ma), during a succession of rift-thermal subsidence episodes, and was terminated during a regional basin-inversion event at ~500 Ma (the Delamerian Orogeny) which deformed and metamorphosed both the Mesoproterozoic basement and its Neoproterozoic cover sequence (e.g. [24]). In the region of the Mount Painter province, the cover sequence thickens towards the south and west from ~7 km near the Babbage Inlier in the north to ~11 km near the southwestern part of the Painter Inlier [25]. Delamerian deformation resulted in shortening of ~20% and the propagation of large amplitude, basement-cored, upright folds [25]. The southwestern part of the basement inlier defines the west-plunging Arkaroola anticline which folds the basement-cover unconformity on a regional scale (Fig. 7). In this area, isograds in the lower part of the cover succession are essentially concordant with the basement unconformity and indicate a dramatic increase in grade towards

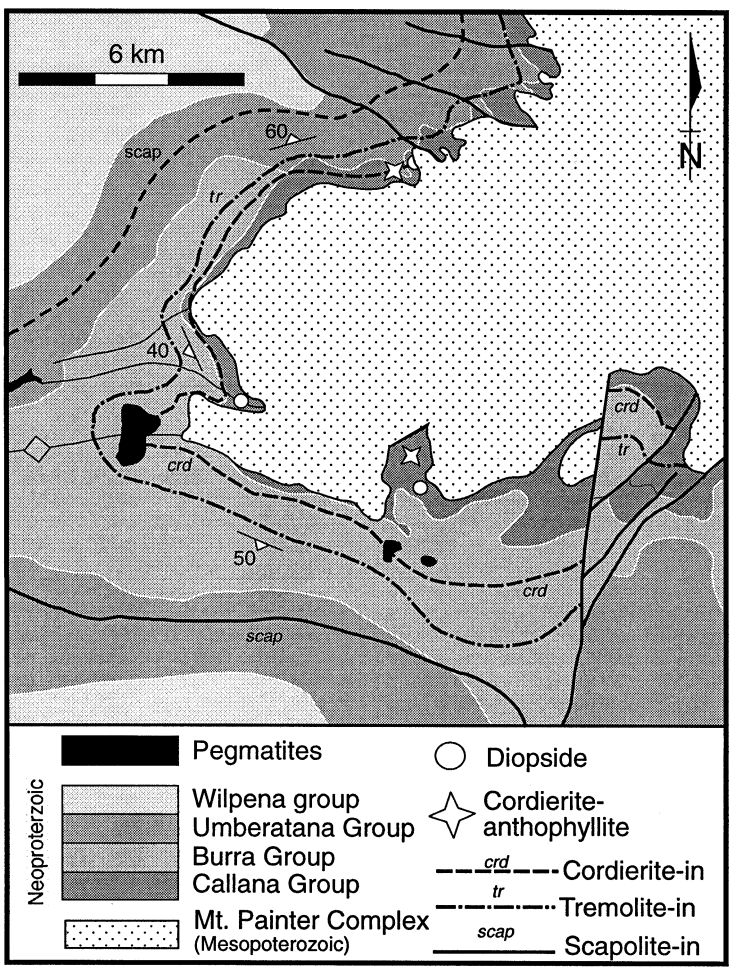

Fig. 7. Geological map of the southwestern Mount Painter Inlier in the northern Flinders Ranges. Isograds are essentially concordant with the unconformity between the Mesoproterozoic Mt. Painter Complex and the Neoproterozoic Adelaidian sequences. Maximum temperatures adjacent to the unconformity are estimated to ~500ºC and pressures in the order of 3 kbar. The pegmatites are locally derived tourmaline-rich derived S-type bodies.

the unconformity [26]. The isograds defining this unique style of 'unconformity related contact metamorphism' are marked by the progressive appearance (in rocks of suitable composition) of scapolite, tremolite, cordierite and diopside. The presence of cordierite–anthophyllite and diopside-bearing rocks immediately above the unconformity indicates temperatures of at least 500ºC. Metamorphic pressures are less well constrained but the widespread association of cordierite–biotite–muscovite is consistent with pressures of about 3 kb, which suggests that the principal mode of burial was achieved by the deposition of the Neoproterozoic cover, and that the average vertical thermal gradient above the currently exposed section was ~50ºC/km.

The Painter Inlier is a U-rich province mined for radium during the Second World War. The basement granitic gneisses of the basement inlier are exceptionally good heat producers, as is reflected in the results of airborne radiometric surveys (Figs. 8 and 9). XRF whole rock analyses from the Mines and Energy South Australia database (along with our own analyses) indicate heat production rates for many of the granitic gneisses in excess of 10 $\mu W\ m^{-3}$, and locally as much as ~50 $\mu W\ m^{-3}$ (Table 2). The mean and median heat production rates (recalculated

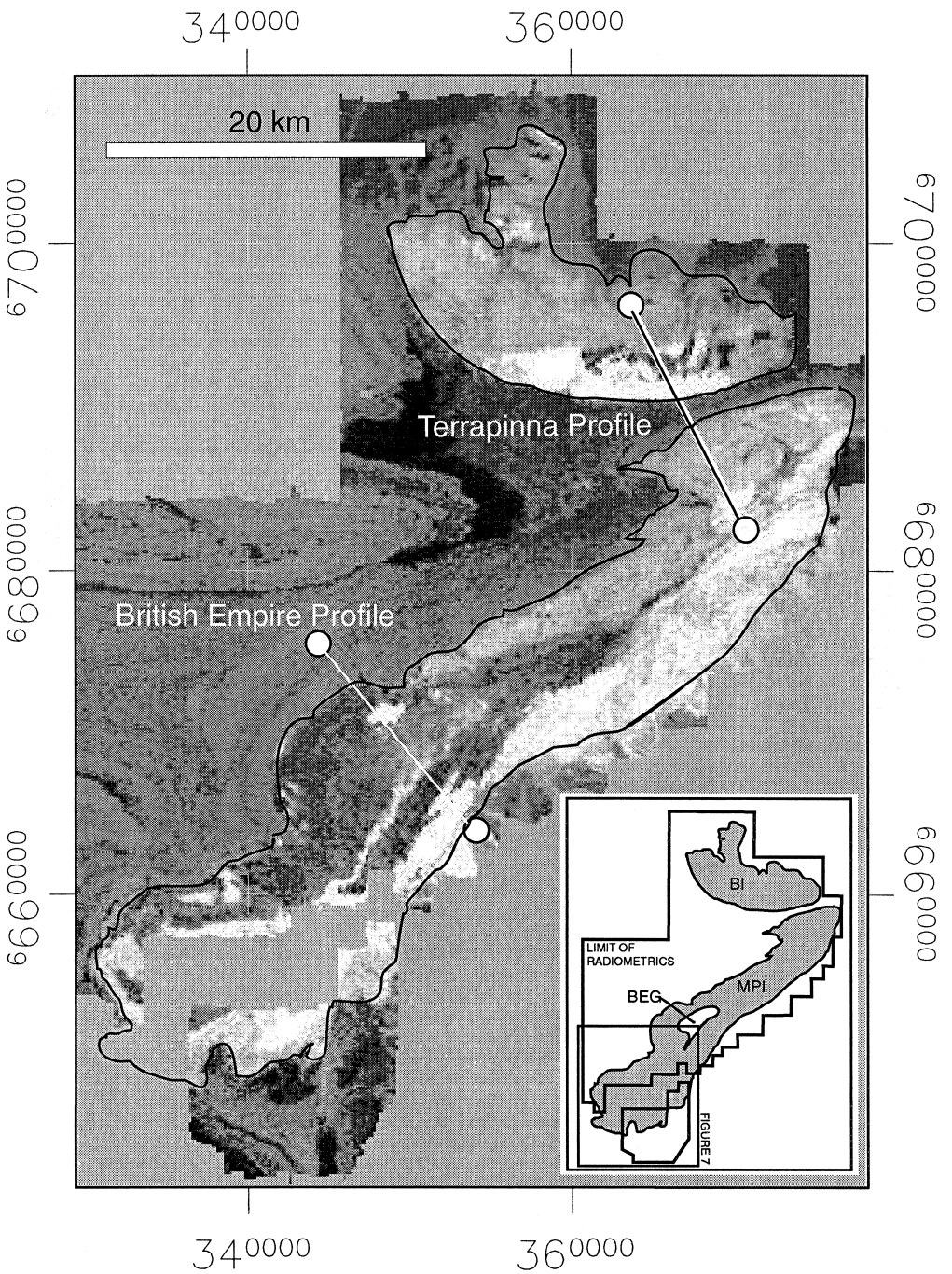

Fig. 8. Grey-scale image showing total counts from airborne radiometric survey. Data courtesy of South Australian Department of Mines and Energy. Poor calibration of this survey precludes direct conversion of the airborne data to effective heat production. Mean K_2O (wt%), Th (ppm) and U (ppm) from XRF analyses of selected rock types are listed in Table 1, along with heat production rates recalculated to 470 Myr (data from the Mines and Energy South Australia geochemical database and our own analyses). Profile data are shown in Fig. 9. High heat production levels are represented by light shades.

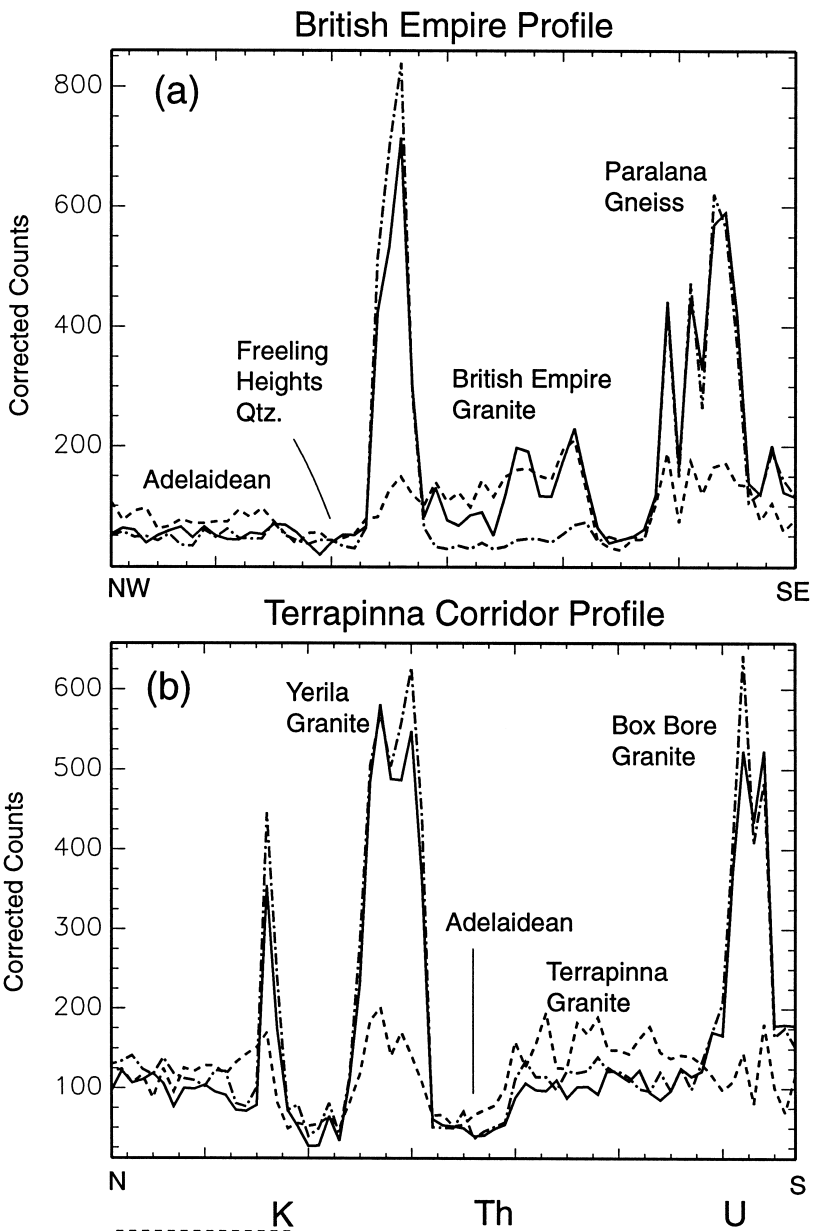

Fig. 9. Total count profile data for the Mount Painter radiometric survey data shown in Fig. 8. Mean K_2O (wt%), Th (ppm) and U (ppm) from XRF analyses of named rock types are listed in Table 1.

at 470 Ma) for both basement granitic and metasedimentary gneisses are 16 and 8 $\mu W\ m^{-3}$, respectively, with an area integrated estimate of the mean heat production for the basement inlier of 9.9 $\mu W\ m^{-3}$ (Table 2). The basement inliers occupy anticlinal culminations ~3 km in amplitude indicating the high heat production layer is of significant thickness. The mean heat production of the overlying sedimentary sequence (15 samples) is 2.6 $\mu W\ m^{-3}$ (recalculated at 470 Ma). Along with the generally elevated heat flows averaging ~85 mW m^{-2} [17], the Painter Inlier heat production rates reinforce the notion parts

Table 2
Heat production parameters for the Painter and Babbage Inliers, northern Flinders Ranges, South Australia

Rock	Area (km^2)	Area (%)	K_2O (wt%)	Th (ppm)	U (ppm)	# [a]	H [b] 470	H^* [c]
Terrapinna granite	99	13	5.4	60	15	12	9.2	1.2
British Empire granite	23	3	4.9	11	16	9	5.9	0.18
Yerila granite	30	4	5.3	333	81	19	48	1.8
Paralana gneiss	22	3	3.3	264	103	30	49	1.4
Mt. Neill granite	189	24	4.9	62	19	20	10	2.4
Felling Heights quartzite	147	19	2.0	7.1	1.8	3	1.2	0.22
Radium Creek metasediments	93	12	4.1	13	7.4	6	3.4	0.41
Box Bore granite	40	5	7.1	108	36	19	19	0.97
Babbage gneisses	144	18	6.1	32	13	8	6.8	1.3
Total	787							9.9

[a] # = number of samples used to derive mean concentrations of K_2O, Th and U.
[b] H = heat production recalculated at 470 My in $\mu W\ m^{-3}$.
[c] H^* = Area normalised heat production representing the contribution of the formation to the mean heat production of the Mesoproterozoic Inliers. The estimated mean heat production of the Inliers at 470 My is 9.9 $\mu W\ m^{-3}$.

of the Australian Proterozoic crust is extraordinarily enriched in heat producing elements. Indeed, a 5 km thick section of the Mt. Painter basement sequence would exceed McLennan and Taylor's [20] estimate for upper limit to the range of crustal contributions to continental heat flow (i.e., 48 $\mu W\ m^2$).

The high heat production rates observed in the Painter Inlier are reflected in a single surface heat-flow record of 126 mW m^{-2}. This heat flow measurement forms part of a broader region of elevated heat-flow through the Flinders Ranges and the adjacent Stuart Shelf and eastern Gawler Craton [17,27], where some 11 measurements fall in the range 72–126 mW m^{-2} with a mean of ~85 mW m^{-2}. As noted earlier, seismic evidence points to relatively thick (~250 km) lithosphere throughout this region [18]. The implied low contemporary mantle heat fluxes (~10–15 mW m^{-2}) imply that elevated surface heat-flows are dominated by crustal contributions; with q_c as much as 110–120 mW m^{-2} for the Painter Inlier, and ~70 mW m^{-2} for many other parts of the Flinders Ranges heat flow province.

The elevated heat production in granitic gneisses occurs throughout the Painter and Babbage Inliers, suggesting a spatial dimension to this heat production anomaly of at least 60 km in the NE–SW direction and at least 35 km in the NW–SE direction. Interestingly, the next structural culmination along the western continuation of the Arkaroola anticline, some 30 km west of map region shown in Fig. 7 and centred some 60 km from the central parts of the Mount Painter Inlier, shows no evidence for elevated metamorphic grades observed in the lower parts of the cover sequence. This suggests that heat production rates in the underlying basement are rather less than at Mount Painter. If this interpretation is correct it implies the heat production anomaly in the Mount Painter region has a characteristic length scale of the order of 50 km and is superimposed on a regional heat flow field significantly lower than at Mount Painter. By analogy with the results of Houseman et al.'s [27] detailed study of heat flow around the Roxby Downs U–Au–REE mine on the Stuart Shelf, some 200 km west of Mount Painter, we might expect regional background surface heat flows of ~75 mW m^{-2}, implying q_c (background) of ~60 mW m^{-2}.

In view of the extremely high geothermal gradients needed to generate the conditions of metamorphism recorded in the Mount Painter province, the question arises as to the nature of the thermal regimes at deeper crustal levels. These deeper crustal thermal regimes can be constrained (at least to the first order level) from deductions based on the presence (or absence) of magmatism. A number of Delamerian granites are known from the Mount Painter region, with all but one forming very small plugs no more than ~50 m in diameter. None show

any systematic relation to the metamorphic isograd structure (Fig. 7). The only Delamerian magmatic body of significant size is the British Empire granite (Fig. 8), which occurs as a sub-horizontal sheet within metasedimentary gneisses near the centre of the Painter Inlier. The British Empire granite is a heterogeneous, per-aluminous granite locally showing ghost-layering parallel to bedding in the enclosing metasediments. This observation and the complex interfingering and gradational contacts with the enclosing, partly migmatitic metasediments is indicative of local derivation. The absence of evidence for any magmas from deep crustal sources suggests the conditions required for significant crustal melting were only locally exceeded at depths close to the current exposures. If this interpretation is correct it implies the ~50ºC/km upper crustal thermal gradients during metamorphism cannot extend much deeper than the presently exposed crustal levels. Average mid-lower crustal thermal gradients of less than about 15ºC/km would be required to keep temperatures at depths appropriate to the Moho (~30 km) lower than ~900ºC.

6. Discussion and conclusions

In the previous sections we have demonstrated that providing the pre-existing crust is sufficiently enriched in heat producing elements, then HGGM in the upper-mid crust will occur as a consequence of thermal subsidence. The important role played by subsidence is twofold. Firstly, because thermal subsidence promotes burial of the 'hot' crust, it naturally increases the depth extent of the high geothermal gradients, potentially inducing very significant temperature increases during progressive burial. Secondly, the lithospheric thickening that drives thermal subsidence reduces the heat flowing into the deeper crust from the mantle. The decrease in the thermal gradients in the deep crust accompanying burial severely limits the temperature changes affecting in the deeper crust (which may cool while the mid-upper crust is heated). We have shown that the necessary geological requirements for HGGM of a thick sedimentary blanket accumulated during rift-subsidence cycles, and a very radioactive basement sequence exist in the Mount Painter province of the northern Flinders Ranges. In this region prima facie evidence for an unusual style of HGGM metamorphism is present in the form of unconformity–concordant isograds, implying average upper crustal thermal gradients at the time of metamorphism of ~50ºC/km.

As far as we are aware, the Mount Painter province provides the best candidate for HGGM due to thermal subsidence. However, we believe this scenario may have broader applicability (see also [15,31]). One of the important facets of the model presented here is that there is no requirement for the thermal events to be transient. Rather, since the thermal regimes are tied to the burial depths of the enriched basement, the duration of metamorphism should reflect the time-scales of burial and exhumation of this basement. In the Mount Painter province, thermal subsidence was terminated by basin inversion during the Delamerian Orogeny. During this event, the isograds were folded and, we presume, the terrane exhumed and cooled. Unusually lengthy durations of metamorphism have been reported from several HGGM terranes (e.g. [11,12]). These studies have been problematic when viewed in terms of the conventional advective heat transport paradigm for such metamorphism. In the example cited by Williams et al. [12] in the Reynolds Range of the Arunta Complex in central Australia, an additional problem for the advective paradigm is that HGGM metamorphism postdates voluminous granitic magmatism by some 200 Myr (see also [14]). These granitic rocks in the Reynolds Range region are particularly good heat producers, averaging some 8 μW m^{-3} when recalculated at the time of metamorphism (see [16]), and are widely distributed, forming some 70% of exposure over an area in excess of 3000 km^2. Carboniferous sediment derived from the subsequent erosion of this basement terrain contains a number of sub-economic U-deposits indicating the crust above the present exposure level was also a good heat producer. The burial of this extensive, high heat production basement during the Proterozoic subsequent to granite emplacement provides an ideal opportunity to develop thermal regimes appropriate to HGGM. A similar situation may hold in the Mount Isa region, where the spatial association between HGGM and very large, 'hot' batholiths such as the Sybella Batholith (e.g., [28]), is at odds

with geochronological data that imply a >120 Myr time lag between granite emplacement and metamorphism [13]. The Sybella Batholith has an average heat production of about 7 μW m^{-3} and horizontal dimensions of some 150 by 30 km. Generally elevated heat production rates throughout the region are indicated by background modern-day heat flows of ~80 mW m^{-2} [17] together with evidence for very thick lithosphere implying low mantle heat flows [18]. Emplacement of the Sybella Batholith appears to have been contemporaneous with rift phase sedimentation and the initial stages of thermal sag [13,29], which together saw the accumulation of >7 km of sediment [30]. Little detail is known of the total thickness of the stratigraphic section that accumulated in the ~120 Myr period between the main rifting and HGGM, some of which was eroded following the basin inversion event that accompanied and terminated metamorphism. However, in view of the thick syn-rift deposits [30] it seems reasonable to assume considerable thermal subsidence prior to metamorphism. Our analysis shows that such subsidence would, at very least, provide a significant thermal priming for the subsequent high geothermal gradient metamorphism.

Acknowledgements

We thank Narelle Neumann for the compilation of the geochemical data listed in Table 2, and Mines and Energy South Australia for providing the geochemical and radiometric survey data summarised in Figs. 8 and 9 and Table 1. We thank Geoff Fraser, Rebecca Jamieson and Page Chamberlain for their reviews of the manuscript. ***[CL]***

References

[1] D.R. Lux, J.J. DeYoreo, C.V. Guidotti, E.R. Decker, Role of plutonism in low-pressure metamorphic belt formation, Nature 323 (1986) 795–797.

[2] M. Sandiford, R. Powell, Deep crustal metamorphism during continental extension; modern and ancient examples, Earth Planet. Sci. Lett. 79 (1986) 151–158.

[3] M. Sandiford, R. Powell, Some remarks on high temperature–low pressure metamorphism in convergent orogens, J. Metamorph. Geol. 9 (1991) 333–340.

[4] V.B. Sisson, L.S. Hollister, T.C. Onstott, Petrologic and age constraints on the origin of a low pressure/high temperature metamorphic complex southern Alaska, J. Geophys. Res. 94 (1989) 4392–4410.

[5] J.J. DeYoreo, D.R. Lux, C.V. Guidotti, Thermal modelling in low-pressure/high-temperature metamorphic belts, Tectonophysics 188 (1991) 209–238.

[6] W.J. Collins, R.H. Vernon, Orogeny associated with anticlockwise P–T–t paths: Evidence from low-P, high-T metamorphic terranes in the Arunta Inlier, central Australia, Geology 19 (1991) 835–838.

[7] M. Sandiford, N. Martin, S. Zhou, G. Fraser, Mechanical consequences of granite emplacement during high-T, low-P metamorphism and the origin of 'anticlockwise' PT paths, Earth Planet. Sci. Lett. 107 (1991) 164–172.

[8] D.M. Winslow, P.K. Zeitler, C.P. Chamberlain, L.S. Hollister, Direct evidence for a steep geotherm under conditions of rapid denudation, western Himalaya, Pakistan, Geology 22 (1994) 1075–1078.

[9] R.W.H. Butler, N.B.W. Harris, A.G. Whittington, Interactions between deformation, magmatism and hydrothermal activity during active crustal thickening; a field example from Nanga Parbat, Pakistan Himalayas, Mineral. Mag. 61 (1997) 37–52.

[10] K.R. Chamberlain, S.A. Bowring, Proterozoic geochronologic and isotopic evolution in NW Arizona, J. Geol. 98 (1990) 399–416.

[11] K.V. Hodges, W.E. Hames, S.A. Bowring, $^{40}Ar/^{39}Ar$ age gradients in micas from a high-temperature–low-pressure metamorphic terrain; evidence for very slow cooling and implications for the interpretation of age spectra, Geology 22 (1994) 55–58.

[12] I.S. Williams, I.S. Buick, I. Cartwright, An extended episode of early Mesoproterozoic metamorphic fluid flow in the Reynolds Range, central Australia, J. Metamorph. Geol. 14 (1996) 29–47.

[13] K.A. Connors, R.W. Page, Relationships between magmatism, metamorphism and deformation in the western Mount Isa Inlier, Australia, Precambrian Res. 71 (1995) 131–154.

[14] J. Vry, W. Compston, I. Cartwright, SHRIMP II dating of zircons and monazites: reassessing the timing of high-grade metamorphism and fluid flow in the Reynolds Range, northern Arunta Block, Australia, J. Metamorph. Geol. 14 (1996) 566–587.

[15] C.P. Chamberlain, L.J. Sonder, Heat-producing elements and the thermal and baric patterns of metamorphic belts, Science 250 (1990) 763–769.

[16] M. Sandiford, M. Hand, Australian Proterozoic high temperature, low-pressure metamorphism in the conductive limit, in: P. Treloar, P. O'Brien (Eds.), What Drives Metamorphism and Metamorphic Reactions? Geol. Soc. London Spec. Publ. 138, 1998, 103–114.

[17] J.P. Cull, An appraisal of Australian heat-flow data, BMR J. Aust. Geol. Geophys. 7 (1982) 11–21.

[18] A. Zielhuis, R.D. Van der Hilst, Upper-mantle shear velocity beneath eastern Australia from inversion of waveforms

from Skippy portable arrays, Geophys. J. Int. 127 (1996) 1–16.
[19] M. Somerville, D. Wyborn, P.N. Chopra, S.S. Raham, D. Estrella, T. Van der Meulen, Hot dry rocks feasibility study, Aust. Energy Res. Dev. Corp. Rep. 94/243 (1994) 133.
[20] S.M. McLennan, S.R. Taylor, Heat flow and chemical composition of continental crust, J. Geol. 104 (1996) 369–377.
[21] E.B. Pereira, V.M. Hamza, V. Furtado, J.A.S. Adams, U, Th and K content, heat production and thermal conductivity of Sao Paulo, Brazil, continental shelf sediments; a reconnaissance work, Chem. Geol. 58 (1986) 217–226.
[22] P. Dovenyi, F. Horvath, A review of temperature, thermal conductivity, and heat flow data for the Pannonian Basin. in: L.H. Royden, F. Horvath (Eds.), The Pannonian Basin; A Study in Basin Evolution, Am. Assoc. Pet. Geol. Mem. 45, 1998, 195–233.
[23] D.P. McKenzie, Some remarks on the development of sedimentary basins, Earth Planet. Sci. Lett. ? (1978) 616–618.
[24] R.F.J. Jenkins, The Adelaide Foldbelt, A tectonic reappraisal, Geol. Soc. Aust. Spec. Publ. 16 (1991) 296–420.
[25] E. Paul, T. Flottman, M. Sandiford, Structural geometry of the northern Flinders Ranges, Aust. J. Earth Sci., 1998, in press.
[26] S. Mildren, M. Sandiford, A heat refraction mechanism for low-P metamorphism in the northern Flinders Ranges, South Australia, Aust. J. Earth Sci. 42 (1995) 241–247.
[27] G.A. Houseman, J.P. Cull, P.M. Muir, H.L. Paterson, Geothermal signatures of uranium ore deposits on the Stuart Shelf of South Australia, Geophysics 54 (1989) 158–170.
[28] M.J. Rubenach, Proterozoic low-pressure/high-temperature metamorphism and an anticlockwise P–T–t path for the Hazeldene area, Mount Isa Inlier, Queensland, Australia, J. Metamorph. Geol. 10 (1992) 333–346.
[29] R. Page, S.-S. Sun, G. Carr, Proterozoic sediment-hosted lead–zinc–silver deposits in northern Australia — U–Pb zircon and Pb isotopic studies (abstract), Aust. J. Earth Sci. 37 (1995) 334–335.
[30] M.G. O'Dea, G.S. Lister, P.G. Betts, K.S. Pound, A shortened intraplate rift system in the Proterozoic Mount Isa terrane, NW Queensland, Australia, Tectonics 16 (1997) 425–441.
[31] L.J. Sonder, C.P. Chamberlain, Tectonic controls on metamorphic field gradients, Earth Planet. Sci. Lett. 111 (1900) 517–535.
[32] A.H. Lachenbruch, Preliminary geothermal model of the Sierra Nevada, J. Geophys. Res. 73 (1968) 6977–6989.